

Heat capacities of LaD_x and LaH_x ($1.9 \leq x \leq 3.0$) from 1 to 300 K

K. Kai

Ames Laboratory, Iowa State University, Ames, Iowa 50011
and The Institute for Materials Research, Tohoku University, Sendai 980, Japan

K. A. Gschneidner, Jr., B. J. Beaudry, and D. T. Peterson

Ames Laboratory and Department of Materials Science and Engineering, Iowa State University, Ames, Iowa 50011

(Received 27 April 1989)

The heat capacities of lanthanum hydrides in the LaD_x and LaH_x ($1.9 \leq x \leq 3.0$) series have been measured over the temperature range from 1.2 to 300 K. The electronic specific-heat coefficients showed nearly the same variation for both LaD_x and LaH_x over the entire composition range, having the values of $\gamma = 0.81 \pm 0.01$ and 0.038 ± 0.01 mJ/g-at. K^2 at the stoichiometric compositions of LaD_2 (LaH_2) and LaD_3 (LaH_3), respectively. Some different variations were found in the composition dependence of the Debye temperatures of the LaD_x and LaH_x series, but, nevertheless, the same values of $\Theta_D = 348 \pm 2$ and 381 ± 2 K were found at the compositions of LaD_2 (LaH_2) and LaD_3 (LaH_3), respectively. The variations of γ and Θ_D do not show a monotonic behavior but depend on the formation of the three hydrogen-ordering phases, namely, $\text{LaD}(\text{H})_{2.25}$, $\text{LaD}(\text{H})_{2.5}$, and $\text{LaD}(\text{H})_{2.75}$. One sharp heat-capacity peak was found in LaD_x between $x = 2.65$ and 2.90 , associated with octahedral hydrogen ordering centered at $\text{LaD}_{2.75}$, whereas four sharp peaks were found in $\text{LaD}_{2.95}$ at 215.5, 265.5, 286.8, and 293.8 K and were correlated with the four transitions observed in LaD_3 by Ito *et al.* The metal-to-semiconductor transition, which is found in the alloys between $2.75 \leq x \leq 3.0$, is discussed on the basis of the electronic specific-heat coefficient and recent theoretical work. We also report that $\text{LaH}_{2.01}$ becomes a superconductor at 0.17 K and, if $\text{LaD}_{2.06}$ goes superconducting, it does so below 0.06 K.

I. INTRODUCTION

In common with the other hydrides of the light lanthanides (i.e., Ce, Pr, and Nd), lanthanum forms a nonstoichiometric hydride phase over a wide composition range of hydrogen from dihydride to trihydride, having a high-symmetry fcc lattice network of La atoms.¹⁻³ The lanthanum hydride system, especially, offers a simple system to study the behavior of hydrogen in a metal lattice and its effect on the electronic properties because it forms a continuous solid solution from $x = 1.9$ to 3.0 and is a nonmagnetic system.^{3,4} The dihydride has the CaF_2 -type structure with hydrogen atoms essentially occupying tetragonal sites (*t* sites). An increase of hydrogen content results in the filling of the octahedral sites (*o* sites) in the fluorite structure up to the trihydride forming the BiF_3 -type structure.¹ However, since these early studies, further developments have shown (1) a premature filling of the *o* sites,^{5,6} for hydrogen content less than LaH_2 , and (2) superstructure phase formation⁷⁻¹⁰ under different conditions of hydrogen content and temperature. A contraction of the lattice is also observed with increasing hydrogen contents from LaH_2 to LaH_3 .^{9,11,12}

Of particular interest is an apparent metal-to-semiconductor (*m-s*) transition, which occurs for hydrogen contents above $x = 2.8$ and, as the temperature is lowered, through 210 K.¹⁰⁻¹⁴

In this investigation, the heat capacities of LaD_x and LaH_x , $1.9 \leq x \leq 3.0$, from 1.2 to 300 K, were measured to

determine the electronic specific-heat coefficient, the Debye temperature, the isotope effect, and the thermodynamic data associated with the phase transitions. These measurements provide new information which is of significance for understanding the structure, electronic states, and *m-s* transition of the lanthanum hydride system.

II. EXPERIMENTAL PROCEDURE

A. Sample preparation

The samples used in this study were prepared starting with the highest purity, Ames Laboratory, polycrystalline lanthanum available. The major metallic impurities in the starting lanthanum were as follows: Si, 30; Fe, 2; Ni, 2.8; Y, 3.1; Ce, 4; Pr, 1; and all other impurities less than 1 in atomic ppm. The major interstitial impurities were as follows: H, 127; C, 23; N, 59; O, 243; and F, 65 in atomic ppm. Two different methods were used to prepare the hydride samples. In the first method, a solid piece of lanthanum which had been electropolished in perchloric acid-methanol solution at 195 K was placed in a platinum boat and reacted with hydrogen or deuterium gas at 400 °C in a conventional pressure-high-vacuum charging system using H_2 or D_2 from a UH_3 or UD_3 gas reservoir, respectively. The concentration of hydrogen or deuterium was determined from the observed quantity of gas absorbed by the sample. The samples prepared by

this method were coarse powders. In the second method, the metal was reacted slowly with H_2 or D_2 mixed with He at 850°C . The lanthanum was wrapped in tantalum foil ($50\ \mu\text{m}$ thick) to prevent reaction with the quartz reaction tube. The H_2 or D_2 was diluted with He to slow the exothermic reaction which would otherwise have raised the sample temperature above the melting point of lanthanum. After the metal was converted to hydride, it was heated at appropriate temperatures between 750 and 900°C under H_2 or D_2 gas pressures from 0.3 to 150 atmospheres to reach the desired composition. The higher reaction temperatures in this method allowed relaxation of the reaction volume changes due to H_2 or D_2 absorption by plastic deformation and resulted in a monolithic, polycrystalline specimen. The composition was determined by a hot vacuum extraction procedure with an accuracy and precision of ± 2 relative percent. The heat-capacity data at a given x value were not affected by the preparation method.

B. Heat-capacity measurement

The low-temperature calorimeter used in this work is of the usual adiabatic heat-pulse type with a mechanical heat switch and a liquid He pot. The sample was loaded into a gold-plated copper holder which was evacuated during the measurements in the low-temperature (1.2 – 20 K) calorimeter. A germanium resistance thermometer was used to measure the temperature between 1.2 and 30 K. The estimated accuracy was ± 0.5 mK in the temperature range from 1 to 5 K and ± 3.0 mK at 20 K. The heat capacity of a 1965 Calorimetry Conference standard copper sample (5.5 g) was measured to serve as a check of the calorimeter. An analysis of the low-temperature heat capacity gave values of 0.692 ± 0.005 mJ/mol K^2 for the electronic specific-heat coefficient and 345.3 ± 1.2 K for the Debye temperature in excellent agreement with 0.694 mJ/mol K^2 and 344.5 K, respectively, for the standard copper sample.¹⁵

Another calorimeter was used for the high-temperature (20 to 300 K) measurements using the same method except that a thermal shield was used around the sample. The sample was placed in another gold-plated copper holder and sealed under a helium atmosphere to keep good thermal contact among the pellets. A Cu/Au-Co thermocouple was used to measure the temperature in the 20 – 77 K range and a copper-constantan thermocouple in the 77 – 350 K range. The thermocouples were calibrated against a standard platinum resistance thermometer. The heat capacity of the 1965 Calorimetry Conference standard copper was measured in the 20 – 300 K range as a check of the calorimeter too, and it was in good agreement with the National Bureau of Standards value¹⁶ with a deviation of less than 1% .

III. RESULTS

A. Low-temperature heat capacity

The heat capacity of the LaD_x ($x=1.91$ – 3.0) and LaH_x ($x=1.90$ – 3.0) samples are shown in Figs. 1(a) and 1(b), and 2(a) and 2(b), respectively. It is noted that each

sample follows a straight line below 4 or 5 K which is about $\frac{1}{50}$ of the Debye temperature, but it begins to deviate from the linear line as the temperature increases. Higher-order terms are associated primarily with dispersions in the phonon spectrum, although they could also be due to deviations from the Debye theory. The heat-capacity data were fitted to the following expression by a least-squares method:

$$C = \gamma T + \beta T^3 + \delta T^5. \quad (1)$$

Here γ is the electronic specific-heat coefficient associated with the electronic density of states at the Fermi energy, β the lattice specific-heat coefficient related to the limiting Debye temperature Θ_D by the relation $\beta = (12\pi^4 R/5)(1/\Theta_D)^3$, with R being the gas constant, and δ is the coefficient to higher-order term.

In the present work, the heat capacity is analyzed in units of mJ/g at. K instead of mJ/mol K [where $1\ \text{mol} = (1+x)\text{g at.}$ for an alloy of the LaH_x composition] because the measured β gives the true Debye temperature using the above expression for β . The coefficients mentioned above are summarized in Tables I and II. The electronic specific-heat coefficient and the Debye temperature are plotted as a function of hydrogen concentration

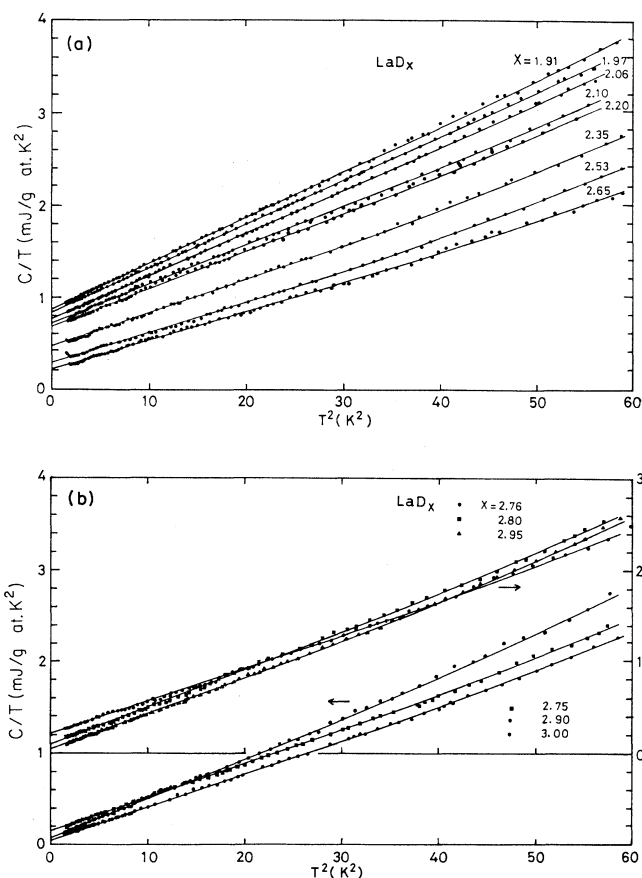


FIG. 1. Low-temperature heat capacities of LaD_x : (a) $1.91 \leq x \leq 2.65$ and (b) $2.76 \leq x \leq 3.0$.

TABLE I. Heat-capacity fit parameters for the LaD_x alloys.

Composition x	γ $\left[\frac{\text{mJ}}{\text{g at. K}^2} \right]$	β $\left[\frac{\text{mJ}}{\text{g at. K}^4} \right]$	δ $\left[\frac{10^4 \text{ mJ}}{\text{g at. K}^6} \right]$	Θ_D (K)
1.91	0.878±0.001	0.048 77±0.000 09	0.23±0.01	341
1.97	0.851±0.001	0.046 27±0.000 17	0.29±0.03	347
2.06	0.776±0.002	0.043 61±0.000 11	0.48±0.02	354
2.10	0.724±0.004	0.041 21±0.000 48	0.25±0.09	361
2.20	0.663±0.002	0.041 63±0.000 38	0.38±0.08	360
2.35	0.467±0.003	0.037 29±0.000 19	0.77±0.02	373
2.53	0.288±0.002	0.030 72±0.000 13	0.93±0.01	398
2.64	0.223±0.002	0.029 14±0.000 14	0.79±0.02	405
2.75	0.157±0.001	0.034 90±0.000 09	0.78±0.01	381
2.76	0.218±0.004	0.033 42±0.000 2	0.73±0.02	387
2.80	0.094±0.004	0.038 93±0.000 2	0.79±0.02	368
2.90	0.078±0.002	0.041 92±0.000 26	0.54±0.06	359
2.95	0.053±0.002	0.035 80±0.000 1	1.0±0.01	378
3.0	0.041±0.004	0.035 56±0.000 12	0.92±0.05	379

x in Figs. 3 and 4, respectively.

First, we will discuss the heat-capacity parameters for the stoichiometric dihydride and trihydride and then the region between these two compositions. The electronic specific-heat coefficient in the LaD_x system decreases in a linear fashion from 0.89 to 0.66 mJ/g at. K² as x varies from 1.91 to 2.20 (Fig. 3). The value of γ for LaH_x shows the same dependence upon the hydrogen concentration in the range of $x = 1.9$ –2.2 as that for LaD_x , although there is some scatter in the data. Thus, both systems do not show any meaningful difference in the electronic specific-heat coefficient over the above-mentioned concentration range including the stoichiometric dihydride. On the other hand, Θ_D increases in a linear fashion from 340 to 400 K as x varies from 1.91 to 2.60 in the LaD_x system, and from 345 to 385 K as x varies from 1.95 to 2.70 in the LaH_x system (Fig. 4). However, the Debye temperature of both stoichiometric dihydrides,

LaD_2 and LaH_2 , have the same value. Thus, we find the electronic specific-heat coefficient and the Debye temperature to be 0.81 ± 0.01 mJ/g at. K² and 348 ± 2 K, respectively, for both LaD_2 and LaH_2 .

Although neither γ nor θ_D show a monotonic variation over the entire region from the dihydride to the trihydride as shown in Figs. 3 and 4, γ decreases linearly in the range between $x = 2.9$ and 3.0, and reaches the same value of $\gamma = 0.038 \pm 0.01$ mJ/g at. K² at stoichiometric LaD_3 and LaH_3 . On the other hand, Θ_D initially decreases as x increases from 2.6 and 2.7 for LaD_x and LaH_x systems, respectively, to reach a minimum value at $x = 2.9$ and then increases again to reach the same value of $\Theta_D = 381 \pm 2$ K at stoichiometric LaD_3 and LaH_3 . The previously reported data for the electronic specific-heat coefficient and the Debye temperature (measured by Ito *et al.*¹⁷) were $\gamma = 0 \pm 0.04$ mJ/g at. K² and $\Theta_D = 241.5 \pm 0.08$ K for LaH_3 , and $\gamma = 0 \pm 0.06$ mJ/g at. K²

TABLE II. Heat-capacity fit parameters for the LaH_x alloys.

Composition x	γ $\left[\frac{\text{mJ}}{\text{g at. K}^2} \right]$	β $\left[\frac{\text{mJ}}{\text{g at. K}^4} \right]$	δ $\left[\frac{10^4 \text{ mJ}}{\text{g at. K}^6} \right]$	θ_D (K)
1.90	0.890±0.002	0.059 53±0.000 22	0.10±0.05	319
1.97	0.772±0.002	0.045 37±0.000 21	0.21±0.05	349
2.10	0.770±0.003	0.044 82±0.000 38	0.15±0.09	351
2.23	0.652±0.002	0.041 35±0.000 35	0.53±0.05	360
2.30	0.553±0.002	0.038 02±0.000 14	0.89±0.01	371
2.50	0.299±0.002	0.036 37±0.000 27	0.05±0.06	376
2.60	0.259±0.003	0.036 69±0.000 46	0.18±0.1	375
2.70	0.191±0.002	0.035 08±0.000 27	0.39±0.06	381
2.75	0.144±0.002	0.034 35±0.000 29	0.63±0.06	383
2.80	0.097±0.003	0.035 69±0.000 37	0.39±0.08	379
2.90	0.058±0.002	0.038 26±0.000 19	0.92±0.03	370
2.95	0.060±0.003	0.036 45±0.000 07	0.57±0.06	376
3.0	0.035±0.003	0.034 85±0.000 11	0.50±0.09	382

and $\Theta_D = 246.3 \pm 0.2$ K, for LaD_3 . But their data included some inaccuracies for the heat capacity of addenda and resulted in a substantially lower value of Θ_D compared with the present data. Regardless, one should note that no isotope effect was observed for either Θ_D or γ with respect to H and D at the stoichiometric dihydride and trihydride compositions.

The hydrogen concentration dependence of the electronic specific-heat coefficient is divided into five stages including the formation processes of the dihydride and trihydride. The first stage corresponds to the process of continuously and randomly filling o sites in the CaF_2 structure to reach $\text{LaD}_{2.2}$ or $\text{LaH}_{2.2}$ while maintaining the CaF_2 structure. The fifth stage is the process of forming LaD_3 or LaH_3 with BiF_3 structure, i.e., the complete filling of the rest of the o sites. The second ($2.2 \leq x \leq 2.45$), third ($2.45 \leq x \leq 2.6$), and fourth ($2.6 \leq x \leq 2.9$) stages are attributed to the formation of the hydrogen-ordering phases with a hydrogen content corresponding to $\text{LaH}_{2.25}$, $\text{LaH}_{2.5}$, and $\text{LaH}_{2.75}$, respectively, which will be discussed in detail in Sec. IV.

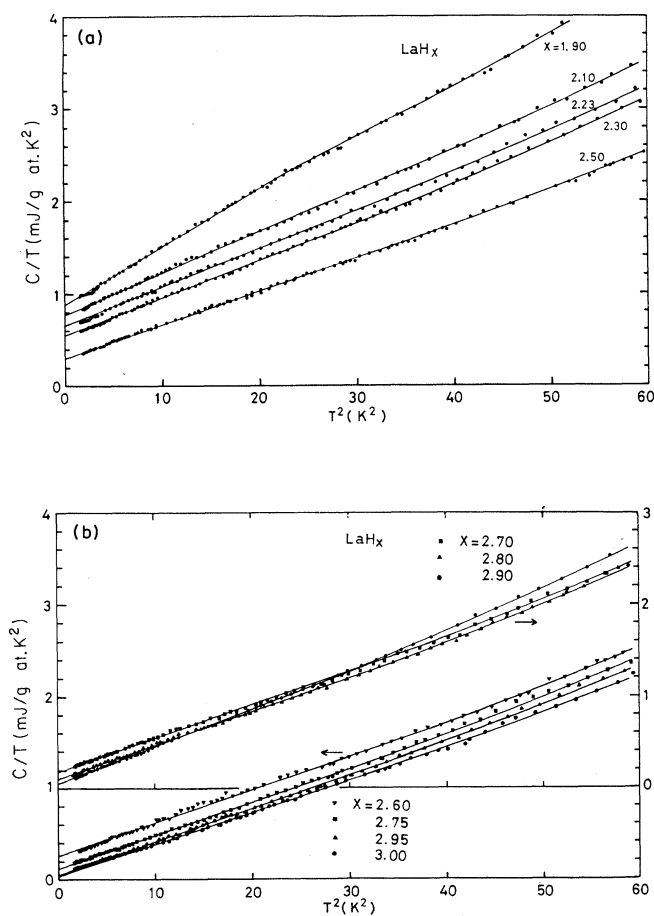


FIG. 2. Low-temperature heat capacities of LaH_x : (a) $1.9 \leq x \leq 2.5$ and (b) $2.6 \leq x \leq 3.0$.

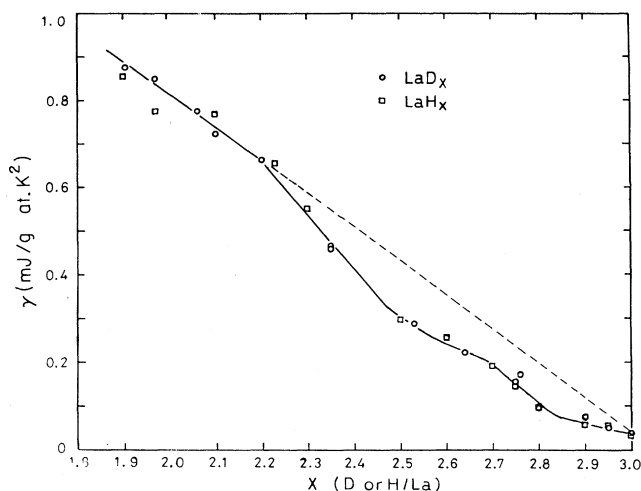


FIG. 3. Plot of electronic specific-heat coefficient γ as a function of hydrogen concentration for LaD_x and LaH_x . See the text for an explanation for the dashed line drawn between $x=2$ and $x=3$.

B. High-temperature heat capacity

The heat-capacity measurements in the range 20–300 K were performed on the six samples with deuterium contents of $x=2.65, 2.75, 2.76, 2.80, 2.90,$ and 2.95 in the LaD_x system. The heat capacities of $\text{LaD}_{2.65}, \text{LaD}_{2.75}, \text{LaD}_{2.80},$ and $\text{LaD}_{2.90}$ are shown in Fig. 5. Only one sharp peak was found at ~ 250 K for these samples. The peak profile and the transition temperature are almost the same as the previous results reported for $\text{LaD}_{2.76}$ and $\text{LaD}_{2.91}$ by Ito *et al.*¹⁸ who attributed the peak to a tetragonal to cubic transition on heating by combining their results with their colleague's x-ray diffraction data.¹¹ On the other hand, two strong peaks are observed at 265.5 and 286.8 K and two weak peaks at

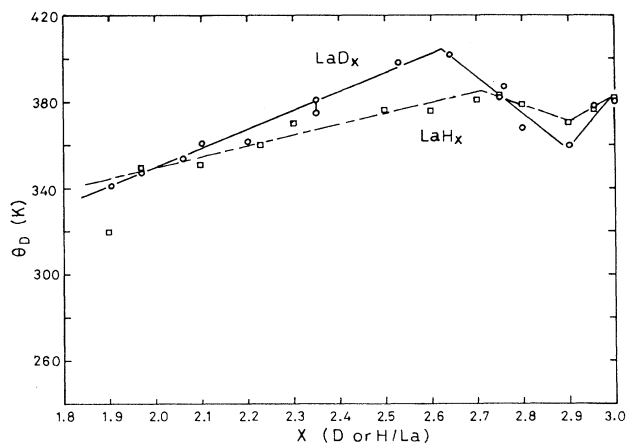


FIG. 4. Plot of the Debye temperature Θ_D as a function of hydrogen concentration for LaD_x and LaH_x .

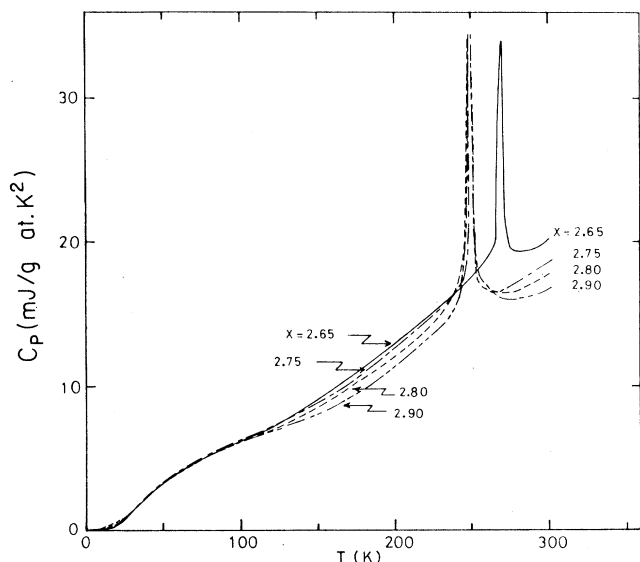


FIG. 5. Heat capacities of four LaD_x alloys for $2.65 \leq x \leq 2.9$ from 1.2 to 300 K.

215.5 and 293.8 K for $\text{LaD}_{2.95}$ as shown in Fig. 6 [the heat-capacity data for LaD_3 (Ref. 17) are included for comparison]. This aspect of the transitions is different from the ones observed in the concentration range of

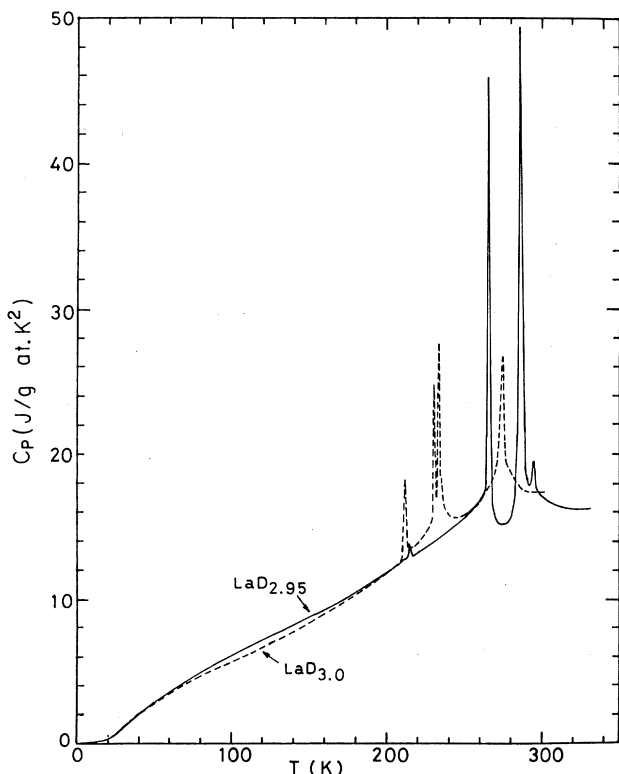


FIG. 6. Heat capacity of $\text{LaD}_{2.95}$ from 1.2 to 300 K. The data of LaD_3 is taken from Ito *et al.* (Ref. 17) and is shown as a dashed line for a comparison.

$x = 2.65$ – 2.9 mentioned above, or from the one with four peaks at 211, 230.5, 233.5, and 274 K for LaD_3 .¹⁷ This will be discussed in more detail in Sec. IV.

The dependence of $S_{298.15}^0$ and $(H_{298.15}^0 - H_0^0)/T$ on the deuterium concentration are shown in Fig. 7, where $S_{298.15}^0$ is the absolute entropy at the temperature of 298.15 K, and $H_{298.15}^0$ and H_0^0 are the enthalpies at 298.15 and 0 K, respectively. The thermodynamic quantities have a plateau at $x < 2.65$ followed by continuous decrease with increasing hydrogen concentration up to $x = 2.9$. This suggests the existence of a phase boundary between alloys with $x < 2.65$ and the hydrogen-ordered phase with $2.65 < x < 2.9$. This is consistent with the low-temperature x-ray study¹¹ in which tetragonal splittings of the cubic diffraction peaks have been observed for the alloys between $\text{LaD}_{2.7}$ and $\text{LaD}_{2.86}$, while no such distortion has been observed down to 30 K for $\text{LaD}_{2.62}$. The other flat part of the concentration dependence of the thermodynamic functions which occur between $\text{LaD}_{2.9}$ and LaD_3 is also consistent with the absence of the apparent tetragonal splitting of cubic peaks when one increases the hydrogen concentration beyond $x = 2.91$.

The entropy of the tetragonal to cubic transformation, ΔS_T^0 versus the hydrogen concentration x is tabulated in Table III together with the other reported data.^{17,18} The fact that the maximum value of ΔS_T^0 (0.87 J/g at. K) lies in the vicinity of $x = 2.75$ indicates that an ordering octahedral hydrogen with a preference towards the c axis

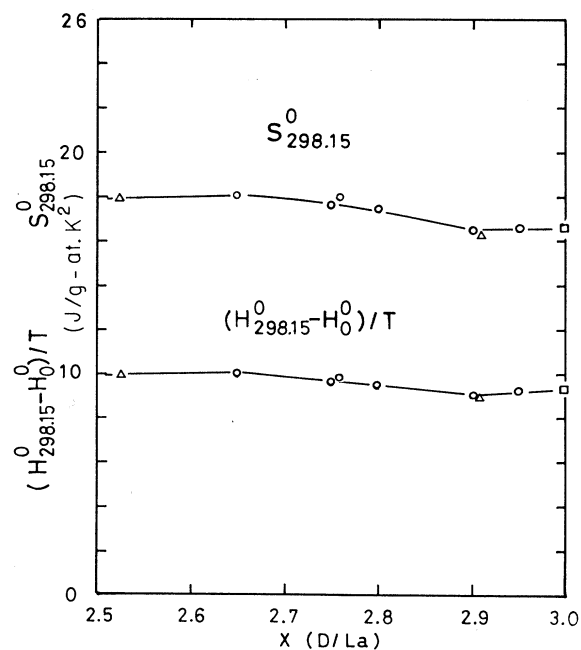


FIG. 7. Absolute entropy at 298.15 K, $S_{298.15}^0$, and the thermodynamic quantity $(H_{298.15}^0 - H_0^0)/T$ dependence on deuterium concentration for LaD_x for $2.53 \leq x \leq 3.0$. The open circles \circ are data from this study, and the squares \square and the triangles \triangle are taken from the results of Ito *et al.*, Refs. 17 and 18, respectively.

TABLE III. Transformation temperatures and entropies of transformation for LaD_x system.

Composition x	Transformation	Transformation temperature (K)	Entropy of transformation (J/g at. K)	Refs.
2.53	No transformation			18
2.65	α - β	269.4	0.388	This work
2.75	α - β	251.5	0.87	This work
2.76	α - β	250.6	0.793	This work
2.80	α - β	247	0.541	This work
2.91	α - β	251.3	0.603	This work
2.91	α - β	251	0.832	18
2.95	I	215.5	0.012	This work
	II	265.5	0.18	
	III	286.8	0.353	
	IV	293.8	0.027	
3.0	I	211	0.053	17
	II	230.5	0.083	
	III	233.5	0.112	
	IV	274	0.176	

occurs in the neighborhood of $x = 2.75$ in LaD_x and results in the forcing of the small tetragonal distortion [1% at maximum (Ref. 11)] in the lanthanum sublattice.

The dependence of the onset transformation temperature on the hydrogen concentration for LaD_x is presented in Fig. 8 together with the other specific-heat data¹⁸ and the x-ray data.¹¹ The transformation temperature

shows a shallow minimum around $x = 2.8$ and slowly rises from $x = 2.8$ to 2.65 with decreasing hydrogen concentration. This behavior seems to be considerably different from that of the LaH_x system in which the transformation temperature falls steeply down to 197 K at $x = 2.6$ with decreasing concentration from $x = 2.8$, according to the x-ray data¹¹ and the specific-heat data.^{19,20} The boundary of the hydrogen-ordered phase centering at $\text{LaD}_{2.75}$ seems to shift to a relatively lower concentration than that for $\text{LaH}_{2.75}$. We will discuss this point in detail in Sec. IV.

IV. DISCUSSION

The specific heat of $\text{LaH}_{2.03}$ has been measured by Bieganski *et al.*²¹ But their electronic specific-heat coefficient $\gamma = 2.82$ mJ/g at. K² (originally reported as 8.54 mJ/mol K²) is significantly larger than the present value of 0.81 mJ/g at. K², while their Debye temperature $\Theta_D = 351$ K (originally and erroneously reported as 243 K because they did not correct for the number of atoms per formula unit to calculate Θ_D when using mJ/mol K units for the heat capacity), agrees with our result of $\Theta_D = 348$ K. One notes that their plot of C/T versus T^2 is not linear below 5.5 K and deviates upward with decreasing temperature. Although the authors gave no explanation for this behavior, this anomaly could result from magnetic impurity elements, such as Fe or magnetic lanthanides, in their sample (no chemical analysis was given). This curvature could lead to a γ value larger than the true one. Recently, some reliable measurements of the low-temperature heat capacity of other dihydrides have been made also using the highest purity rare-earth metals available, as prepared by Materials Preparation Center of the Ames Laboratory. The values of γ and Θ_D have been determined to be 0.68 ± 0.02 mJ/g at. K² and 710 ± 10 K, respectively, for ScH_2 ,²² 0.66 ± 0.02 mJ/g at.

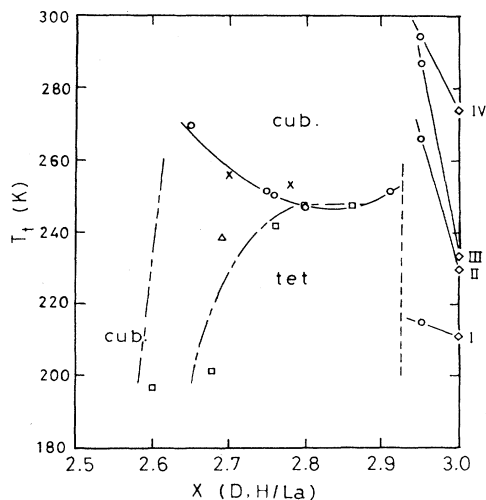


FIG. 8. Transformation temperature vs the deuterium (—) and hydrogen (---) concentrations: \times and \square are taken from the x-ray study (Ref. 11) of the LaD_x and LaH_x systems, respectively, and \triangle is from the heat-capacity data for $\text{LaH}_{2.69}$ (Refs. 19 and 20). The open circles \circ are data from this study, except for LaD_3 (\diamond) which are taken from Ito *et al.* (Ref. 17). The lines (—) and (---) are the suggested phase boundaries between the compositions $\text{LaD}_{2.50}$ and $\text{LaD}_{2.75}$, and between the compositions $\text{LaD}_{2.75}$ and LaD_3 , respectively.

K^2 and 525 ± 10 K, respectively, for YH_2 ,²² and 0.724 ± 0.002 mJ/g at. K^2 and 361.4 ± 0.3 K, respectively, for LuH_2 .²³ These values are compared to those of their respective pure metals, namely, 10.334 ± 0.011 mJ/g at. K^2 and 345.3 ± 1.0 K for Sc metal,²⁴ 7.878 ± 0.004 mJ/g at. K^2 and 244.4 K for Y metal,²⁴ 9.45 ± 0.02 mJ/g at. K^2 and 150 ± 1 K for La metal,²⁵ and 8.194 ± 0.016 mJ/g at. K^2 and 183.2 ± 0.3 K for Lu metal,^{23,24} where all the metals are in the hcp form except for La which has the dhcp structure. When one takes the ratio of the γ values for the dihydride to the ones for the pure metal (in the same manner as in Ref. 26) in order to verify if the value of γ for $\text{LaH}_{2.03}$ obtained by Bieganski *et al.*²¹ is too large, the above mentioned data gives a ratio of 0.066, 0.084, 0.086, and 0.088 for ScH_2 , YH_2 , LaH_2 , and LuH_2 , respectively. The ratio for ScH_2 :Sc is low because of the large spin-fluctuation enhancement of the γ value for Sc.²⁴ Furthermore, the ratio of the Θ_D for the dihydride to the one for the pure metal gives values of 2.06, 2.15, 2.32, and 1.97 for ScH_2 , YH_2 , LaH_2 , and LuH_2 , respectively. These nearly constant ratios for γ and Θ_D for the four dihydrides indicate that the previously reported value of γ for $\text{LaH}_{2.03}$ (Ref. 21) is substantially in error. Therefore, there is now no significant discrepancy²⁶ for the γ value for LaH_2 compared with those of the other dihydrides.

Since Switendick's pioneering work,²⁷ the realistic calculations of the electronic structure have been performed on a few of the lanthanide dihydrides. Gupta and Burger²⁸ have performed a nonself-consistent band calculation of the electronic structure using an augmented-plane-wave (APW) method for fcc LaH_2 and LaH_3 . The calculated total density of states for LaH_2 have several features which are noted as follows. The low-lying hydrogen-metal bonding states are separated by an indirect gap of 0.118 Ry from the upper band and the states are essentially composed of lanthanum d character wave functions. The low-lying bands are filled by four of the five valence electrons of LaH_2 and the remaining electron fills the metal $5d$ band. The Fermi level, therefore, falls just above the bottom of the $5d$ band below a sharp peak at $E = 0.447$ Ry. The density of states (DOS) at the Fermi energy E_F was $N(E_F) = 15.05$ states for both spins/Ry unit cell.²⁸

Misemer and Harmon²⁶ have presented the most complete self-consistent calculations for LaH_2 and LaH_3 , including relativistic effects which are important for heavier elements where the eigenvalues and eigenvectors were found using the Korringa-Kohn-Rostoker (KKR) method. The calculated band structure for LaH_2 roughly agrees with the results after Gupta and Burger,²⁸ but Misemer and Harmon found a rather small value for $N(E_F) = 11.6$ states for two spins/Ry unit cell at $E = 0.55$ Ry as expected since they had broader bands than those calculated by Gupta and Burger. Another self-consistent but nonrelativistic band-structure calculation found $N(E_F) = 14.5$ states for two spins/Ry unit cell at $E = 0.50$ Ry.²⁹ Our experimental electronic specific heat $\gamma = 0.81$ mJ/g at. K^2 yields a DOS value of 12.4 states for two spins/Ry unit cell taking account of the

calculated electron-phonon enhancement factor²⁸ of $\lambda = 0.13$. This low λ value is also consistent with the low superconducting temperature of 0.17 K for our $\text{LaH}_{2.10}$ sample, and < 0.06 for $\text{LaD}_{2.06}$, if it does become a superconductor.³⁰ Therefore, the value of $N(E_F) = 11.6$ states for two spins/Ry unit cell derived by Misemer and Harmon²⁶ is the most reasonable theoretical one for the bare density of states at the Fermi energy.

Next, we interpret the concentration dependence of the electronic specific heat between LaH_2 and LaH_3 . There are, so far, no theoretical calculations for the variation of the electronic structure with hydrogen concentration increasing from dihydride to trihydride, but it is helpful to deduce the variation of the electronic states by comparing the results of band calculations for LaH_2 and LaH_3 .²⁶ The hydrogen $1s$ state couples preferentially to La d orbitals with t_{2g} symmetry and hence yields a charge-density maxima along $\langle 111 \rangle$ directions, which point toward the t sites. On the other hand, the La d orbitals with e_g symmetry are directed toward $\langle 100 \rangle$ directions in which the o sites are located.²⁶ If one increases the hydrogen concentration from LaH_2 , the metal d bands with t_{2g} symmetry are depleted to form the two low-lying bonding states coupled with the hydrogen atom on the t site, and only the metal d band, which is simply formed by one band with e_g character, remains below the Fermi energy. With a further increase of hydrogen atoms on the o site, a third bonding band is formed below the metal d bands so that the bands with e_g character retained near the bottom of the metal d bands are completely depleted at the Fermi energy to form the LaH_3 . LaH_3 is, therefore, a semiconductor or semimetal because the three low-lying bands are nearly completely filled with the six valence electrons in the trihydride in agreement with the resistivity^{12,31} and NMR data³² or the present specific-heat measurement. Therefore, it is suggested that the metal derived band with e_g character is continuously depleted by adding hydrogen atoms onto the o site. Thus the decrease of the DOS of the metal d band at the Fermi energy could be proportional to the hydrogen concentration added to the o site.

In our model, the composition dependence of the electronic specific-heat coefficient is given as a linear dashed line drawn between the experimental γ 's for LaH_2 (LaD_2) and LaH_3 (LaD_3) in Fig. 3. This simple idea reproduces the slope of the γ versus x line established over the $1.9 \leq x \leq 2.2$ range. The deviations from the ideal line are due to the three superstructure phases which have been claimed to exist under substantially different conditions of temperature and compositions.³³⁻⁴¹ These superstructure phases are assumed to be formed at the compositions $\text{LaH}_{2.25}$, $\text{LaH}_{2.5}$, and $\text{LaH}_{2.75}$ on the basis of the following critical review of the literature.

The existence of long-range order in $\text{CeD}_{2.15}$ has been claimed on the basis of neutron diffraction³³ and subsequently, a tetragonal structure ($I4_1md$) (Refs. 34 and 35) was proposed for the ordered $\text{LaD}_{2.3}$, $\text{CeD}_{2.29}$, and $\text{PrD}_{2.37}$. Knappe and Muller *et al.*^{9,36,37} have also reported the existence of the tetragonal phases for $\text{RH}_{2.33}$ ($R = \text{La, Ce, Pr, Nd, and Sm}$) which they assigned the

space group $I4_1md$. Samples with hydrogen concentration $x < 2.38$ were found to be cubic. Neutron diffraction,¹⁰ DTA (differential thermal analysis) analysis,^{38,39} and deuterium NMR (Ref. 40) have shown that these phases are actually two different superlattices. One type of the ordered phase of the tetragonal structure with space group $I4_1md$ was found at compositions near $x = 2.43$, whereas another tetragonal ordered phase with the space group $I4/mmm$ was assigned to an alloy having the ideal stoichiometry of $x = 2.25$.¹⁰ In the NdH_x system ($2.1 < x < 2.8$), two phase transformations were observed which were characterized by the presence of a dome-shaped maxima around the concentrations corresponding to $x = 2.25$ and 2.50 .³⁷ The transition temperature for the phase attributed to $I4/mmm$ symmetry increases from 235 K for $x = 2.12$ –370 K for $x = 2.34$ and the other phase with $2.4 < x < 2.5$, the temperature could be lowered to less than 290 K.³⁹ The deuterium magnetic resonance (DMR) (Ref. 40) for LaD_x gave additional evidence for the existence of the two tetragonal phases: one appropriate to $\text{LaD}_{2.25}$ and the other to $\text{LaD}_{2.50}$. Furthermore, they noted that the quadrupole splitting of the spectrum becomes weak with increasing temperature and disappears at 250 K. But a puzzling feature of these materials is that both x-ray¹¹ and the high-temperature heat-capacity¹⁸ measurements were unsuccessful in observing a tetragonal distortion of the lanthanum lattice for $\text{LaH}_{2.53}$ and $\text{LaD}_{2.53}$ compositions.

Turning back to the paper of Fedotov *et al.*¹⁰ for solving this puzzle, we note that the second superlattice phase is limited to a relatively narrow range of RD_x ($R = \text{a rare-earth metal}$, $x = 2.37$ – 2.48) which is at a lower concentration than $RD_{2.5}$, whereas the first superlattice phase exists over a wide range of concentration of $x = 2.15$ – 2.37 . These results are analogous to the NdH_x phase diagram obtained by DTA measurements.³⁹ Approximately 3% of the tetrahedral sites of these superlattices are vacant and, as a result, an enhanced number of o sites are filled at the expense of the vacant t sites.^{7,39} Therefore, the ideal octahedral content necessary to form the superlattice $RD_{2.50}$ can be attained near $RD_{2.43}$. This phenomenon could be caused by thermal hydrogen excitation from a t site into an o site, the activation energy of which can depend on concentration.³⁸ The continued introduction of additional deuterium atoms beyond $x = 2.43$ could lower the ordering temperature such that the dome-shaped maximum of the t - o transformation temperature versus composition plot is shifted to a lower concentration from ideal stoichiometry of $x = 2.50$. The rapid lowering of the hydrogen-ordering temperature is expected to occur around the composition of $\text{LaD}_{2.53}$ where the t - o transition was not detected by x-rays.¹¹ The variation of the entropy of transformation with concentration also supports this as is evident by the rapid decrease on the low-concentration side of $\text{LaD}_{2.75}$ (see Table III). It is, therefore, concluded that the superlattice phase with $I4_1md$ is centered at $x = 2.43$ – 2.48 and that the stoichiometric $\text{LaD}_{2.50}$ remains cubic.

The low-temperature heat capacities indicate that there is no essential difference for the γ values between

LaD_x and LaH_x systems. The absence of an isotope effect on the electronic specific-heat constant can be explained using two different models, similar to the way the isotope effect on the superconducting temperature of PdD(H) is explained. The first model involves the influence of the optic mode on the electron-phonon coupling force on D or H sites.⁴² The second model attributes the effect to the difference in the electronic structure through the different anharmonicities in the potential of H or D.⁴³ Klavins *et al.*¹¹ have measured the lattice constants of LaH_x and LaD_x over the concentration range $2.0 \leq x \leq 3.0$. Their extrapolated values for $x = 2.0$ and 3.0 are identical to within 0.2% for the deuteride and hydride. Considering the small difference for the lattice parameters, we can regard the band structures of the deuteride and hydride as identical. But if there is a difference, that should be attributed to the difference of the electron-phonon enhancement factors λ_D and λ_H through the D and H optic phonons. The La site contribution λ_{La} , however, remains identical for the hydride and deuteride. The calculated electron-phonon enhancement factor is $\lambda = 0.13$ for LaH_2 (Ref. 28) in agreement with the low superconducting temperature of $\text{LaH}_{2.1}$, as mentioned above. This small value suggests a small anharmonicity of the D or H motion over the harmonic potential compared to the larger value⁴² found in PdD(H) , implying essentially no isotope effect. There is the possibility that an isotope effect can be observed in the trihydride deuteride, in which a third of the deuterium (or hydrogen) occupy the octahedral site, because the electron may feel more pronounced anharmonicity around such a site. However, the experimental γ value is too small to distinguish an isotope effect.

Upon the addition of hydrogen, the La Knight shift⁴⁴ and the quantity $(T_2 T)^{-1/3}$ with respect to the proton spin-relaxation^{45,46} decrease and simultaneously the electrical resistivity^{12,47} rises substantially as o sites are occupied beyond $x = 2.7$ in LaD_x and LaH_x . Not only is there a concentration-dependent m - s transition, but also a temperature-dependent m - s transition as the hydrogen concentration is increased from $x = 2.7$ to $x = 3$. These behaviors correspond to the rapid decrease in the electronic specific-heat coefficient near $x = 2.75$, as shown in Fig. 3, indicating a decrease in the electronic density of the states at the Fermi energy.

Resistivity data on $\text{LaH}_{2.49}$ taken by Finnemore and Manzini³¹ show a metallic behavior both below and above the 270 K transition. The resistivity decrease can be ascribed to an ordering of the hydrogens in o sites, similar to that observed in the classical order-disorder transition of Cu_3Au . However, the electrical conduction changes from metallic to semiconducting at $x > 2.7$ and, simultaneously, a resistivity jump (increase) is found. There is about a factor-of-3 jump for the samples with $2.7 < x < 2.8$ in CeH_x at the hydrogen-ordering temperature⁴⁷ at $T = 245$ K. For this type of concentration-dependent m - s transition, a Mott-type mechanism has been proposed and is ascribed to the formation of a defect band due to the unoccupied o sites for $x < 3$ in LaH_x versus the case where the o sites were completely occu-

pied to form the semiconductive LaH_3 .^{46,48} According to the electronic structure calculation by Fujimori and Tsuda,⁴⁹ the narrow defect band at E_F , which is formed below the bottom of the conduction band, is half occupied, corresponding to one electron per one octahedral hydrogen vacancy. The defect level acts as an electron donor and the reduction in the density of states due to the reduction of the octahedral vacancy is responsible for the decrease of γ as a function of x for $x \geq 2.75$ (see Fig. 3).

The resistivity data for the higher concentration sample $\text{LaH}_{2.86}$, however, revealed a different behavior from the conduction scheme mentioned above; that is, a semiconductive behavior above and below the 195 K transition temperature. Note that this temperature is much lower than that of the tetragonal lattice transition, but rather close to 210 K temperature, below which a substantial decrease of the Knight shift³² and at which the m - s transition peak of the heat capacity¹⁷ have been observed in LaD_3 . Although we could not detect a heat-capacity peak ascribed to the m - s transition near 200 K in $\text{LaD}_{2.9}$, the four peak anomalies as found in LaD_3 were observed in $\text{LaD}_{2.95}$, including the m - s transition at 217 K (see Figs. 6 and 8). In fact, the entropy change due to the tetragonal-to-cubic transformation in $\text{LaD}_{2.9}$ appears to be relatively larger than that expected from the decreasing trend from $x = 2.75$ to $x \approx 2.9$ (see Table III). This indicates that the $\text{LaD}_{2.9}$ sample is slightly deuterium deficient relative to the nominal concentration, or that the $\text{LaD}_{2.86}$ sample studied by Ref. 31 could contain more deuterium than they supposed. In any case, the four sharp heat-capacity peaks found in $\text{LaD}_{2.95}$ (I, II, III, and IV, at 215.5, 265.5, 286.8, and 293.8 K, respectively), clarify the existence of the phase boundary between $x = 2.86$ and 2.95, although the phase boundary cannot be clearly determined. A phase diagram for LaD_x and LaH_x is proposed, as shown in Fig. 8, on the basis of the above discussion. We can safely conclude that the appearance of the temperature-dependent m - s transition (and also semiconductor-to-semiconductor) for $x > 2.9$ is accompanied by the formation of a phase isomorphous with LaD_3 (the four sharp heat-capacity peaks), while the m - s transition for $2.75 < x < 2.9$ is induced by the cubic-to-tetragonal transition.

The suggested m - s transition at 210 K, corresponding to transformation peak I in LaD_3 is accompanied by the

random localized displacements of the octahedral deuterium atom from the true center to the off-center positions along $\langle 111 \rangle$ directions below 230 K, corresponding to the specific-heat peak II.¹⁷ This transition temperature appears to rise up to ~ 270 K in the deuterium deficient $\text{LaD}_{2.95}$. Kulikov and Zvankov⁵⁰ pointed out that the Coulomb interaction between an electron pocket near the L point and a hole pocket near the Γ point, based on the semimetallic Fermi surface of lanthanum trihydride, results in a charge-density wave along the $\langle 111 \rangle$ directions which then drives the second-order transformation from semimetal to an excitonic insulator state below the critical temperature. This could explain why the temperature-dependent m - s transition for $x > 2.9$ is independent of the tetragonal distortion which induces a m - s transition for $2.7 \leq x \leq 2.9$, since the octahedral hydrogen displacements of the on-center to off-center positions, due to the appearance of the charge-density wave, could retain cubic structure in LaD_3 ,¹⁷ and maybe in $\text{LaD}_{2.95}$ too.

In addition to these unusual behaviors, band-structure calculations show a semimetallic band in which the top of the valence band overlaps the bottom of the conduction band for LaH_3 and predict a nonzero value of $\gamma = 0.14$ mJ/g at K^2 . These calculations are consistent with the experimental result of a finite electronic specific-heat coefficient for LaH_3 or LaD_3 , although the theoretical value is substantially larger than our result of $\gamma = 0.038$ mJ/g at K^2 . Misemer and Harmon,²⁶ however, found a much smaller indirect gap of 0.2 mRy between Γ and L than the values of 29 mRy reported by Kulikov and Zvonkov,^{29,50} and 41 mRy by Gupta and Burger.²⁸ The indirect gap or band overlap is very sensitive to the potential approximation used and a tendency for a smaller value appears if one improves the approximation of the crystal potential.⁵⁰ To elucidate such a subtle band structure for LaH_3 we will have to await further calculations.

ACKNOWLEDGMENTS

The authors wish to thank Dr. R. G. Barnes and Dr. B. N. Harmon for helpful suggestions and discussions. The authors also thank Mr. A. Johnson for his assistance in preparing some of the lanthanum hydrides. The Ames Laboratory is operated for the U.S. Department of Energy by Iowa State University under Contract No. W-7405-ENG82. This research was supported by the Director of Energy Research, Office of Basic Energy Science.

¹W. M. Muller, J. P. Blackledge, and G. G. Libowitz, *Metal Hydrides* (Academic, New York, 1968), p. 395.

²G. G. Libowitz and A. J. Maeland, *Handbook on the Physics and Chemistry of Rare Earths*, edited by K. A. Gschneidner, Jr. and L. Eyring (North-Holland, Amsterdam, 1979), Vol. 3, p. 299.

³R. R. Arons, in *Hexagonal Ferrites. Special Lanthanide and Actinide Compounds*, Vol. 12c of *Landolt-Börnstein*, New Series, edited by K.-H. Hellwege (Springer-Verlag, Berlin, 1982), p. 372.

⁴B. Stalinski, *Bull. Acad. Polon. Sci., Classe III*, **3**, 613 (1955).

⁵W. A. Kamitakahara and R. K. Crawford, *Solid State Com-*

mun. **41**, 843 (1982).

⁶E. L. Venturini, *Electronic Structure and Properties of Hydrogen in Metals*, edited by P. Jean and C. B. Satterthwaite (Plenum, New York, 1983), p. 97.

⁷A. G. Cheetham and B. E. F. Fender, *J. Phys. C* **5**, L35 (1972).

⁸C. G. Titcomb, A. K. Cheetham, and B. E. F. Fender, *J. Phys. C* **7**, 2409 (1974).

⁹P. Knappe, H. Muller, and H. W. Mayer, *J. Less-Common Met.* **95**, 323 (1983).

¹⁰V. K. Fedotov, V. G. Fedotov, M. E. Kost, and E. G. Ponyatovskii, *Sov. Phys. Solid State* **24**, 1252 (1982) [*Fiz. Tverd. Tela (Leningrad)* **24**, 2201 (1982)].

- ¹¹P. Klavins, R. N. Shelton, R. G. Barnes, and B. J. Beaudry, *Phys. Rev. B* **29**, 5349 (1984).
- ¹²B. Stalinski, *Bull. Acad. Polon. Sci., Classe III*, **5**, 1002 (1957).
- ¹³G. G. Libowitz, *Ber. Bunsenges. Phys. Chem.* **76**, 873 (1972).
- ¹⁴G. G. Libowitz, J. G. Pack, and W. P. Binnie, *Phys. Rev. B* **6**, 4540 (1972).
- ¹⁵D. W. Osbourne, H. E. Flotow, and F. Shreiner, *Rev. Sci. Instrum.* **38**, 159 (1967).
- ¹⁶G. T. Furukawa, W. G. Saba, and M. L. Reilly, *Natl. Bur. Stand. Ref. Data Ser., Natl. Bur. Stand. (U.S.) Circ. No. 18*, (U.S. GPO, Washington, D.C., 1968); G. K. White and S. J. Collocott, *J. Phys. Chem. Ref. Data* **13**, 1251 (1984).
- ¹⁷T. Ito, B. J. Beaudry, K. A. Gschneidner, Jr., and T. Takeshita, *Phys. Rev. B* **27**, 2830 (1983).
- ¹⁸T. Ito, B. J. Beaudry, and K. A. Gschneidner, Jr., *J. Less-Common Met.* **88**, 425 (1982).
- ¹⁹Z. Bieganski and M. Drulis, *Phys. Status Solidi A* **44**, 91 (1977).
- ²⁰Z. Bieganski and B. Stalinski, *Z. Phys. Chem.* **116**, 109 (1979).
- ²¹Z. Bieganski, D. G. Alvarez, and F. W. Klaaijzen, *Physica* **37**, 153 (1967).
- ²²K. Kai, C. H. Chung, K. A. Gschneidner, Jr., and D. T. Peterson (unpublished).
- ²³D. K. Thome, K. A. Gschneidner, Jr., G. S. Mowry, and J. F. Smith, *Solid State Commun.* **25**, 297 (1978).
- ²⁴T.-W. E. Tsang, K. A. Gschneidner, Jr., F. A. Schmidt, and D. K. Thome, *Phys. Rev. B* **31**, 235 (1985).
- ²⁵P. H. Pan, D. K. Finnemore, A. J. Bevolo, H. R. Shanks, B. J. Beaudry, F. A. Schmidt, and G. C. Danielson, *Phys. Rev. B* **21**, 2809 (1980).
- ²⁶D. K. Misemer and B. N. Harmon, *Phys. Rev. B* **26**, 5634 (1982).
- ²⁷A. C. Switendick, *Solid State Commun.* **8**, 1463 (1970); A. C. Switendick, *Int. J. Quantum Chem.* **5**, 459 (1971).
- ²⁸M. Gupta and J. P. Burger, *Phys. Rev. B* **22**, 6074 (1980).
- ²⁹N. I. Kulikov, *J. Less-Common Met.* **88**, 307 (1982).
- ³⁰K. Kai and K. A. Gschneidner, Jr. (unpublished).
- ³¹D. K. Finnemore and S. Manzini (private communication).
- ³²R. G. Barnes, B. J. Beaudry, R. B. Creel, and D. R. Torgeson, *Solid State Commun.* **36**, 103 (1980).
- ³³A. K. Cheetham and B. E. F. Fender, *J. Phys. C* **5**, L35 (1972).
- ³⁴C. G. Titcomb, A. K. Cheetham, and B. E. F. Fender, *J. Phys. C* **7**, 2409 (1974).
- ³⁵J. J. Didisheim, K. Yvon, P. Fischer, W. Halg, and L. Schlappbach, *Phys. Lett.* **78A**, 111 (1980).
- ³⁶H. Muller, P. Knappe, and O. Greis, *Z. Phys. Chem.* **114**, 45 (1979).
- ³⁷P. Knappe and H. Muller, *Z. Anorg. Allg. Chem.* **487**, 63 (1982).
- ³⁸L. O. Bashkin, E. G. Ponyatovskii, and M. E. Kost, *Phys. Status Solidi B* **91**, 401 (1979).
- ³⁹L. O. Bashkin, M. E. Kost, and E. G. Ponyatovskii, *Phys. Status Solidi A* **83**, 461 (1984).
- ⁴⁰D. G. de Groot, R. G. Barnes, B. J. Beaudry, and D. R. Torgeson, *J. Less-Common Met.* **73**, 233 (1980).
- ⁴¹J. Schefer, P. Fischer, W. Halg, J. Osterwalder, L. Schlappbach, and J. D. Jorgesen, *J. Phys. C* **17**, 1575 (1984).
- ⁴²D. A. Papacostantopoulos, B. M. Klein, E. N. Economou, and L. L. Boyer, *Phys. Rev. B* **17**, 141 (1977).
- ⁴³R. J. Miller and C. B. Satterthwaite, *Phys. Rev. Lett.* **34**, 144 (1975).
- ⁴⁴D. S. Schreiber and R. M. Cotts, *Phys. Rev.* **131**, 1118 (1963).
- ⁴⁵D. R. Torgeson, L.-T. Lu, T.-T. Phua, R. G. Barnes, and D. T. Peterson, *J. Less-Common Met.* **104**, 79 (1984).
- ⁴⁶D. Zamir, R. G. Barnes, N. Salibi, R. M. Cotts, T.-T. Phua, D. R. Torgeson, and D. T. Peterson, *Phys. Rev. B* **29**, 61 (1984).
- ⁴⁷G. G. Libowitz and J. G. Pack, *J. Chem. Phys.* **50**, 3557 (1969).
- ⁴⁸G. G. Libowitz, *Ber. Bunsenges. Phys. Chem.* **76**, 837 (1972).
- ⁴⁹A. Fujimori and N. Tsuda, *J. Phys. C* **14**, 1427 (1981).
- ⁵⁰N. I. Kulikov and A. D. Zvonkov, *Z. Phys. Chem.* **117**, 113 (1979).